Reinforcement Learning-based Adaptive Mitigation of Uncorrected DRAM Errors in the Field

Isaac Boixaderas
Barcelona Supercomputing Center
Barcelona, Spain
isaac.boixaderas@bsc.es

Sergi Moré
Barcelona Supercomputing Center
Barcelona, Spain
sergi.more@bsc.es

Javier Bartolome
Barcelona Supercomputing Center
Barcelona, Spain
javier.bartolome@bsc.es

David Vicente
Barcelona Supercomputing Center
Barcelona, Spain
david.vicente@bsc.es

Petar Radojković
Barcelona Supercomputing Center
Barcelona, Spain
petar.radojkovic@bsc.es

Paul M. Carpenter
Barcelona Supercomputing Center
Barcelona, Spain
paul.carpenter@bsc.es

Eduard Ayguadé
Barcelona Supercomputing Center
Universitat Politècnica de Catalunya
Barcelona, Spain
eduard.ayguade@bsc.es

ABSTRACT

Scaling to larger systems, with current levels of reliability, requires cost-effective methods to mitigate hardware failures. One of the main causes of hardware failure is an uncorrected error in memory, which terminates the current job and wastes all computation since the last checkpoint. This paper presents the first adaptive method for triggering uncorrected error mitigation. It uses a prediction approach that considers the likelihood of an uncorrected error and its current potential cost. The method is based on reinforcement learning, and the only user-defined parameter is the mitigation cost. We evaluate our method using classical machine learning metrics together with a cost–benefit analysis, which compares the cost of mitigation actions with the benefits from mitigating some of the errors. On two years of production logs from the MareNostrum supercomputer, our method reduces lost compute time by 54% compared with no mitigation and is just 6% below the optimal Oracle method. All source code is open source.

CCS CONCEPTS

• **General and reference** → **Reliability**; • **Hardware** → **Failure prediction**; • **Computer systems organization** → **Reliability**; **Availability**.

KEYWORDS

Memory system, Reliability, Error prediction, Machine learning, Reinforcement learning, Cost–benefit analysis.

1 INTRODUCTION

System resilience is an important requirement for large-scale clusters, especially in high-performance computing (HPC), where a single job may execute for days on thousands of nodes. If any node fails, the job is terminated, wasting all CPU–hours since the last checkpoint. One of the principal causes of hardware failure in HPC clusters is an uncorrected error (UE) in main memory [25, 29, 30, 56]. A cost-effective DRAM error mitigation scheme will therefore allow us to maintain reliability as we scale to larger systems.

The majority of prior work on prediction of corrected [6, 15, 18, 44, 61] and uncorrected [25, 42, 64] memory errors shows great performance in terms of accuracy, precision, and recall. It is unclear, however, whether these prediction methods can be used as the basis for a memory error mitigation scheme that is cost-effective and useful in practice. Practical cost-effectiveness and usefulness can only be evaluated using a cost–benefit analysis, which compares the resources needed for training, prediction and failure mitigation against the saved compute time due to successful mitigation [11]. Saved compute time is quantified in node–hours, which is the sum across all nodes of the wallclock time (in hours) that would otherwise have been lost. Cost–benefit analysis is complex and dependent on the failure mitigation strategies and HPC job sizes [11, 17]. On a given system, the cost of an uncorrected error varies among jobs whose size and duration can differ by orders of magnitude [23, 27, 48–50, 57, 70, 71], and even within a single job depending on the time since it started or last performed a checkpoint.

To the best of our knowledge, this paper develops and evaluates the first adaptive AI method that decides to trigger the mitigation

action depending on both the likelihood of an error and its potential cost to the current jobs. Our method is based on reinforcement learning (RL), and it takes account of preceding warnings, corrected and uncorrected errors, and node-level events such as reboots. The RL agent decides when to take active measures to mitigate a potential uncorrected error. It is independent of the specific method used for mitigation, so it can be applied to control various approaches such as node cloning, live job migration or checkpointing. The only user-defined parameter is the total mitigation cost, so the method can be applied to other systems without customization or tuning. We release all code as open source [10].

We train and evaluate the model on MareNostrum [3], one of six Tier-0 HPC systems in Europe. At the time of the study, it comprised 3056 nodes with more than 25,000 memory DIMMs. The error logs cover a production period of more than two years, from October 2014 to November 2016, during which we detected 4.5 million corrected errors and 333 uncorrected errors.

The cost–benefit analysis shows a saving of more than 40,000 node–hours over two years, a 54% reduction compared with no mitigation. This saving is just 6% below that of the optimal Oracle prediction scheme. The evaluation starts from an untrained model, and is based on time series cross-validation, in order to avoid overfitting to the fixed historical data [68].

We increase confidence in the generality of the method by showing that it works well for all three major DRAM manufacturers. Evaluation with different mitigation costs indicates that the model could be applicable to different failure mitigation approaches. Finally, the model outperforms other predictors when the job sizes are scaled up to ten times smaller or larger than during MareNostrum production. Applying our method to larger systems would therefore lead to roughly proportional savings that are larger by orders of magnitude.

The rest of the paper is structured as follows. Section 2 describes the environment and collection of the error and job logs. Section 3 explains the Markov decision process formulation of the problem and its solution using a dueling double deep Q-network. Section 4 explains the evaluation methodology and Section 5 gives the results. Section 6 is the related work and Section 7 concludes the paper.

2 ENVIRONMENT DESCRIPTION

2.1 MareNostrum 3 error logs

Our algorithm is trained and evaluated using memory error and job logs from two generations of the MareNostrum supercomputer. The error logs were obtained from MareNostrum 3 [3] over more than two years of production from October 2014 to November 2016. At the time, MareNostrum 3 was one of six Tier-0 (largest) HPC systems in the partnership for advanced computing in Europe (PRACE) [2]. It comprised 3056 compute nodes, each with two eight-core Intel Sandy Bridge-EP E5-2670 sockets and a clock frequency of 2.6 GHz. We use the error logs from the compute nodes, excluding the login and test nodes that are not part of the monitoring infrastructure and whose failures do not affect the compute jobs. The jobs executed on MareNostrum 3 were mainly large-scale scientific HPC applications, and system utilization was generally above 95%. During the observation period, we collected data from more than 25,000 DDR3-1600 DIMMs. We analyze DIMMs from all three major memory manufacturers, which have been anonymized

and are referred to as *Manufacturer A, B* and *C*. There are 6694, 5207 and 13,419 DIMMs from *Manufacturer A, B* and *C*, respectively.

MareNostrum 3 employed single device data correction (SDDC) ECC. The ECC check is performed on each application memory request and by a patrol scrubber which periodically traverses physical memory and performs an ECC check on each location.

2.1.1 Corrected errors (CEs). A daemon, based on mcelog from Linux [34], periodically extracted information related to corrected errors from the Intel CPU machine check architecture (MCA) registers [34]. Each CE was recorded in the log file, specifying the time stamp, node id, DIMM id, and physical location of the error including DIMM rank, bank, row and column.[1] The log entry also indicates whether the CE was found by an application memory read or the patrol scrubber. If there were more than one error within the measured time period, the MCA registers record the number of errors and provide detailed information for only one of the errors. Our logs therefore give the precise number of CE and they provide detailed error information for a subset of the errors. We selected a time period of 100 ms for the daemon, as this was the shortest time period with a negligible performance overhead. A shorter period would increase the size of the sample of detailed error information, but it would also increase the overhead. Previous studies perform readings at a similar [11, 58–60] or larger time period, up to once per hour [37].

2.1.2 Uncorrected errors (UEs). The IBM firmware [31], which is part of the MareNostrum 3 monitoring software, logged uncorrected errors, specifying, for each error, which DIMM failed and whether the UE occurred during an application memory read or it was found by the patrol scrubber. The log also contains critical over-temperature conditions, which similarly cause the node to be shut down, so are counted as equivalent to uncorrected errors. It additionally records UE warnings, generated when the correctable ECC logging limit has been reached or the memory modules are throttled to prevent an over-temperature condition. UE warnings are input features to the algorithm but not counted as UEs.

2.1.3 UE reduction. As is the case for many failure events [26, 55], uncorrected errors tend to appear in bursts [11, 74]. Burstiness is important to consider in any study related to UE prediction or mitigation, especially since, for our dataset at least, the second and subsequent UEs within a burst, which have no effect on system reliability, are much easier to predict than the first UE in a burst. In MareNostrum, whenever a node encountered a UE, it was removed from production and tested for one week. This means that only the first UEs on a node, within a period of one week, have an impact on a production workload. Filtering the dataset to contain only the first UE in each burst (of up to a week), reduced the number of UEs from 333 UEs to 67 UEs, making a major difference to our method's design and evaluation.

2.1.4 DIMM retirement bias. MareNostrum includes a pre-failure alert, which identifies DIMMs that are close to failure. Such DIMMs were retired in order to reduce the incidence of uncorrected errors in the production system. Over the two-year production period, 51 DIMMs were retired by the system administrators. This action

---

[1]The mapping from address to physical location is sensitive manufacturer information, and was obtained using help from a memory manufacturer.

is recorded in the system log with the date and time. We could not determine the specific reasons for DIMM retirement. Surprisingly, most of the retired DIMMs experienced no preceding corrected or uncorrected errors in the error log, and they performed no node boots in the days before the retirement. A recent IBM study [25] mentions hundreds of sensors that are used by the system integrators to predict component failures. We had no access to these sensors in the system under study.

Preventive DIMM retirement introduces a bias in training and evaluation that we were unable to avoid. Since it is impossible to know whether an event followed by DIMM retirement would otherwise have been followed by an uncorrected error, we remove all such samples from training and evaluation.

2.1.5 Quantitative analysis. Zivanovic et al. [74] perform detailed analysis of the same MareNostrum 3 error logs that are used in our study. They apply several different methods for quantitative and statistical analysis of the DRAM corrected and uncorrected errors, as well as memory system faults. The authors also compare the results for different DRAM manufacturers and DRAM cell technologies. The number of UEs in Zivanovic et al. differs from our results by about 6%. This is because they exclude DIMM critical over-temperature conditions and ignore address DIMM retirement bias (Section 2.1.4). Their analysis is a complement to this paper and it gives confidence that the error logs used for our study are representative of typical DRAM failures.

2.2 MareNostrum 4 job logs

The log of the jobs was obtained from the general-purpose block of the successor, MareNostrum 4 [4], which has 3456 nodes, each with two 24-core Intel Xeon Platinum sockets at 2.1 GHz. The job log covers the production period from Mar. 2018 to Mar. 2019. For practical reasons, it was impossible to use error and job logs from the same period and system. We believe that combining logs from different machines and different production time periods does not significantly change any of the conclusions. The process of combining error logs and job logs from both systems is elaborated upon in Section 3.3.3. The only major aspect that could not be addressed in this study is any possible correlation between the occurrence of errors and recorded job characteristics such as wallclock duration and number of nodes.

The job log was collected by Slurm [72], which is the job scheduler used to run jobs on MareNostrum 4. We extracted the log using the sacct command, which provides the job's submission time, start and end times, allocated node IDs, and other information.

3 ADAPTIVE ERROR MITIGATION CONTROL

3.1 Background

Reinforcement learning (RL) is one of the most promising machine learning (ML) approaches for tackling hard control problems. The main difference between RL and other ML methods is that RL learns in a dynamic environment. An RL approach is composed of three main elements: the *agent*, the *environment*, and the *reward function*. The agent interacts with the environment, which is a model of the system, by observing the current state of the environment and taking a specific action. In response, the environment changes the

state and the agent receives a reward. The agent's goal is to discover and take the optimal sequence of actions in the environment in order to maximize the cumulative sum of the rewards. The learned mapping between the states of the environment and the actions is known as the policy. The agent learns, i.e. it updates its policy, by exploring and interacting with the environment.

An RL problem is usually formalized as a Markov decision process (MDP) [8], which has four elements: 1) the set of states of the environment, 2) the set of possible actions, which may depend on the current state, 3) the probabilities of moving among states depending on the action, and 4) the rewards associated with these transitions. Each will be explained in the context of DRAM error mitigation in Section 3.2.

The goal of an RL algorithm associated with an MDP is to find a policy that maximizes the discounted sum of the rewards from each time-step:

$$\sum_t \gamma^t R(t), \tag{1}$$

where γ (gamma) is the discount factor and $R(t)$ is the reward obtained at time t. The discount factor is between 0 and 1, and its value controls the tradeoff between taking an immediate high reward and maximizing rewards over time.

Q-learning [66] is an RL algorithm in which the agent independently learns the value of each action in each state. The value is the expected accumulated reward, from Equation 1, of taking a given action in the starting state and following the learned policy thereafter. All these values, for every possible state and action, are stored in a table known as the Q-function.

Many problems, including DRAM error mitigation, have states with a large number of dimensions, some of which are continuous or have so many values they are effectively continuous. Learning and storing the value of each state individually would be prohibitive in terms of training time and storage, so various approaches are used to approximate the Q-function. One of the best known approaches, deep Q-learning [40], approximates the Q-function using a deep neural network known as a deep Q-network. The agent trains the network to minimize a loss function, which quantifies the error introduced by approximating the Q-function.

We employ two known approaches: dueling double deep Q-network (DDDQN) [65] and prioritized experience replay (PER) [53]. A DDDQN is both a double deep Q-network and a dueling network architecture. A double deep Q-network uses two different neural networks, one to select the action and the other to evaluate it, mitigating a well known overestimation bias due to self-evaluation. A dueling network architecture splits the Q-function into two parts, known as the value function and the advantage function. The value function is the expected reward, according to the policy, in a given state and the advantage function indicates how much better each action is compared with the expected reward. This approach is known to converge more rapidly to an optimal policy [65]. PER stores the outcomes of past experience in the environment, and training is done based not only on the current actions but mini-batches of past experiences. The experiences with higher discrepancies between predicted and actual outcomes are considered more important, guiding the prioritization mechanism so as to improve the efficiency of learning.

Table 1: Features used for UE mitigation control

Feature in state (per node)
Corrected errors (CEs):
Number of corrected errors since the last event
Number of CEs since the beginning of operation*
Number of ranks, banks, columns and rows with CEs
Number of DIMMs with CEs
Uncorrected errors:
Number of UE warnings since the beginning of operation
System state:
Time since the last node boot (start)
Number of node boots*
Workload:
Potential uncorrected error (UE) cost

* Feature variation over time (Equation 2) is calculated for this feature.

3.2 MDP formulation of UE mitigation control

3.2.1 State and features. The features in the state are listed in Table 1. The CE, UE and system state features, i.e. all features except the potential UE cost, are derived from the error log events observed in the nodes of MareNostrum 3. All features are calculated at each time step, and provided directly to the agent. In addition, for the two features annotated with an asterisk, the feature variation over time is calculated as:

$$\textit{Feat. variation }(\Delta t) = \frac{\textit{Feat. value (Prediction moment)}}{\textit{Feat. value (Prediction moment - }\Delta t)}, \quad (2)$$

where Δt is the time increment. The feature variation over time is calculated for Δt equal to 1 minute and 1 hour, and it is set to zero if the denominator in the above equation is zero.

The potential UE cost depends on the workload, and is the total number of node–hours that would have been lost if a UE had occurred at the moment the agent is invoked:

$$UE\_cost = nodes \times \min(\textit{wallclock\_since\_job\_start}, \\ \textit{wallclock\_since\_checkpoint}). \quad (3)$$

3.2.2 Actions. There are always two actions available to the agent: it can either request a job mitigation (action a equals 1) or do nothing (a equals 0).

3.2.3 State transitions. After taking an action, the agent has nothing to do until the next event. If the next event is a UE, then the whole node is shut down and the job is terminated without invoking the agent. Otherwise, the state will transition to correspond to the next event. When the events are taken from a historical log, the CE, UE and system state features and their relative rates of change over time do not depend on the agent's last action. The potential UE cost, however, always depends on whether a mitigation was performed. If the agent did not trigger a mitigation, then the potential UE cost is increased by the job's elapsed node–hours. If the agent requested a mitigation, then the potential UE cost is first set to zero to reflect the mitigation action, and then it is increased by the job's elapsed node–hours. There is a minimum wallclock time between state transitions of one minute, so that events occurring within the same minute are combined. For our system we found that a higher frequency than once per minute would increase the overhead but make no improvement to the cost–benefit analysis.

3.2.4 Reward. The reward function is calculated based on the lost node–hours of the system:

$$R_a = -a \times \textit{mitigation\_cost} - \textit{UE\_occurred} \times \textit{UE\_cost}, \quad (4)$$

where a is the action (1 for a mitigation, 0 otherwise) and *UE_occurred* equals 1 if a UE occurred following the action and 0 otherwise.

3.2.5 Error mitigation actions and cost. The RL agent decides when to perform mitigation actions, based on the error-related features and the potential cost of an error. If the agent requests a mitigation, then the actual error mitigation is performed by the *environment*. As such, the agent is independent of the specific mitigation method, and the only mitigation-related parameter is the mitigation cost.

The training and evaluation in Section 5 uses a error mitigation cost of 2 node–minutes, following estimations from a recent study of Das et al. [17]. The study analyzes various actions that can mitigate the impact of node failures, such as live job migration, node cloning and checkpointing, and concludes that 2 min suffice for most of these actions. We also consider the mitigation cost of 5 and 10 node–minutes, which is the checkpointing time considered in various previous studies [9, 21, 22, 24, 33, 46, 51].

Finally, the UE cost is calculated using Equation 3 with the timestamp of the UE. This means that the UE cost always includes the full time elapsed between the last mitigation and the actual UE. The goal of the agent is to maximize the cumulative discounted sum of these negative costs.

3.3 Solving the Markov Decision Process (MDP)

3.3.1 Overall approach. Figure 1 illustrates how the RL agent solves the MDP problem described in the previous section. The diagram shows the environment on the left and the agent on the right. In our implementation based on historical logs, the environment obtains the UEs, CEs, events and job state from the logs, as described in Section 2. In a real system, the environment would collect this information from the monitoring daemons and workload manager. The environment passes the state to the agent, which supplies the state features to the neural network to determine the action. In order to avoid overestimation of the action values and to learn a better policy, we use a dueling double deep Q-learning neural network. Given the action selected by the agent, the environment either performs a mitigation or it does not. On the next event, it calculates the reward for the last action, depending on the last time that mitigation was performed and whether or not the next event is a UE.

3.3.2 Architecture. As an approximator for the Q-function, the agent uses a deep neural network composed of the input features, four hidden layers with 256, 256, 128, and 64 neurons, respectively, and a single output to indicate whether or not to mitigate.

3.3.3 Training. Training is divided into episodes, each of which is a "run" of the agent in its environment from an initial to a terminal state. In our context, a single node is chosen randomly and the episode runs from the beginning to the end of the split (Section 4.1), taking all events on that node. A sequence of jobs is randomly chosen to run on the node. The jobs are weighted by the number of
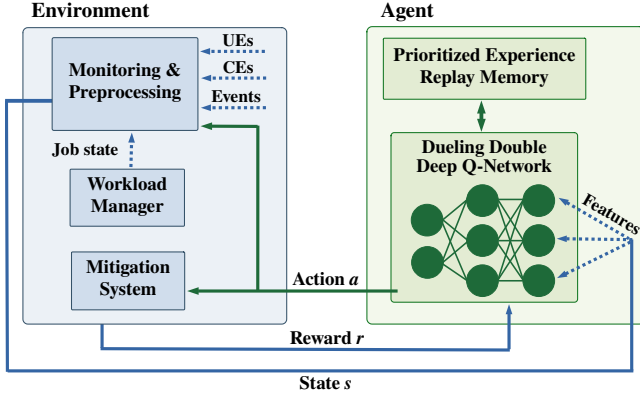
Figure 1: Interaction between RL agent and environment for adaptive UE mitigation.
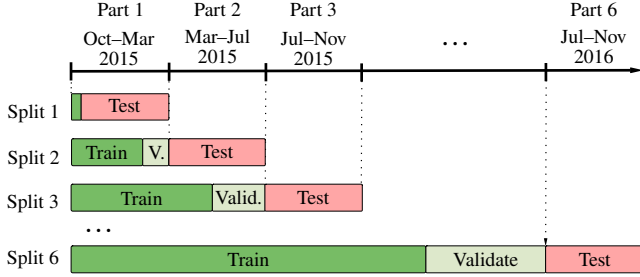

Figure 2: Evaluation using time series nested cross-validation. The error log is divided into six equal parts and evaluation for each split is divided into training (with multiple hyperparame- ters), validation (to find the best hyperparameters), and testing.

nodes on which they execute, in order to maintain the correct job distribution. During training, the agent learns to maximize the reward by improving its future actions based on its current experience.

3.3.4 Class imbalance. During the two-year period, there were 67 UEs (following UE reduction of Section 2.1.3) out of a total of 259,270 events (after merging events in the same minute). This imbalance of 3.5 orders of magnitude between the numbers of UEs and events causes the learning process to be slow. We therefore use a form of experience replay known as prioritized experience replay (PER) [53] (Section 3.1), which speeds up learning by prioritizing experiences that are expected to result in more learning progress. In our case, PER demonstrated effectiveness in handling class imbalance without the need for additional techniques commonly employed in ML for this purpose.

4 EVALUATION METHODOLOGY

4.1 Time series nested cross-validation

We evaluate our RL approach on production data using time series nested cross-validation, which is a well-known technique for determining how well a model performs and generalizes in a setup similar to how it would be used in practice. Figure 2 summarizes this

methodology. The error log is divided into six equal parts (shown horizontally), each of which corresponds to roughly four months of data. These parts are used to create six splits (shown vertically), each of which allows a separate evaluation on a part of the test data, using a model trained with hyperparameters chosen using data that precedes that part. The evaluation for each split is divided into training (with multiple hyperparameters), validation (to find the best hyperparameters), and testing (to evaluate the cost–benefit). Although it is common in RL to only present the results for an agent using the best hyperparameters, our use of historical data rather that an interactive setting means that this approach would introduce bias [68].

In the hyperparameter tuning phase we adjust the learning rate of the neural networks, the discount factor γ, the update and synchronization frequencies of the two networks and some of the parameters of the prioritized experience replay, such as the batch sample size. We perform a first round of random search with 60 sets of hyperparameters, selecting the hyperparameters of the best performing agent on the training data and running another round with a narrowed search space, close to those best hyperparameters, finally selecting the best performing agent on the validation set. Each agent is trained with 20,000 episodes,[2] which proved to be sufficient to achieve stable decisions with good rewards.

Each split, except the first, allocates the first 75% of the time before the new part for training and the remaining 25% for validation. The training set is used to train multiple agents with different hyperparameters, starting from an untrained model for the first split and a mix of previously trained and untrained models for each subsequent split. The validation set is then used to select the best performing agent. If there are no UEs in the validation set, which happens when partitioning by manufacturer due to the low frequency of UEs, then we select the best performing agent for the training set. This introduces some bias but it avoids the risk of choosing a weak mitigation policy. The best agent is then evaluated using the testing dataset. The testing dataset is then incorporated into the training and validation datasets of the next part, which is again divided in the same ratio of 75% to 25%. The first split is slightly different, because it employs the first two weeks from the log for both training and validation, and the rest of the first three-month part is used for testing. This approach allows us to include almost all of the production log in the evaluation. The overall result is the total node–hours lost, due to mitigations and UEs, accumulated across all six splits used for evaluation.

4.2 Approaches under evaluation

We evaluate six prediction-based approaches that can be used to decide when to perform UE mitigation:

- *Never-mitigate* does not initiate any UE mitigation. It leads to the maximum possible UE cost but the minimum possible mitigation cost.
- *Always-mitigate* triggers a UE mitigation for every event in the error log. It has the minimum possible UE cost but the maximum possible mitigation cost, among policies that signal mitigations only when there is an error event. It is

---

[2]Although the error and job logs are fixed historical records, each episode is different because it uses a random sequence of jobs (Section 3.3.3).

implicitly a form of predictor, since an event in the error log is treated as an indicator of an upcoming UE.

- *SC20-RF* is the state-of-the-art random forest (RF) predictor of Boixaderas et al. [11]. The authors applied six machine learning classifiers and found that random forest, with random under-sampling to address class imbalance, provided the best results. The output of the random forest predictor is a value from 0 to 1 that represents the probability of an uncorrected error. A mitigation is triggered if the value exceeds an externally provided threshold parameter. We start from an untrained model, but provide maximum advantage to SC20-RF by using the optimal threshold parameter.
- *SC20-RF-2%* and *SC20-RF-5%* are the SC20-RF policy with realistic (suboptimal) values of the threshold parameter, differing from the optimal value by 2% and 5% respectively.
- *Myopic-RF* is an extension of *SC20-RF* that adapts to the current potential UE cost. It triggers a mitigation action if the expected cost from a UE (probability of a UE multiplied by the cost it would have), without mitigation, is greater than the cost of mitigation. The probability of a UE is estimated by the RF predictor.
- *RL* is the reinforcement learning approach presented in this paper, always starting from an untrained model.
- *Oracle* signals a UE mitigation on the last event before each UE. It therefore performs the minimum number of mitigations necessary to predict the maximum number of UEs. It is the optimal strategy assuming that all mitigations are performed following events in the log. It is not a realistic policy for implementation, but it allows us to quantify the room for improvement.

4.3 Total costs in node–hours

All cost–benefit calculations show the total number of lost node–hours, i.e. the sum of the UE cost and mitigation cost. The UE cost is computed using Equation 3, calculated at the precise time of each UE. The mitigation cost is the total cost of the mitigation actions plus, for SC20-RF, Myopic-RF and RL, the cost of all training and validation used to create the model. The time to determine the optimal threshold parameter for SC20-RF is not included in the evaluation.

There is a 7% difference between our results for SC20-RF in Section 5 and the results in its original publication [11]. This is because the previous study does not compute the lost compute time between the mitigation action and a UE, when a UE occurs inside the prediction window (period for which the prediction is made). Our results always count the full UE cost, including the full time period between the last mitigation action and the UE.

4.4 Classical machine learning metrics

Previous studies that propose error prediction methods [11, 15, 18, 25, 61, 64] are evaluated using standard prediction metrics such as recall or precision. For completeness, and to allow a direct comparison with these methods, we also evaluate our RL method using these standard metrics.

In order to perform this evaluation, we classify the actions of the prediction-based methods as:

- **True positives (TPs)**: Number of UEs that were mitigated.

- **False negatives (FNs)**: Number of UEs that were not mitigated.
- **False positives (FPs)**: Number of mitigations minus the number of TPs.
- **True negatives (TNs)**: Number of non-mitigations minus the number of FNs.

Following Boixaderas et al. [11], the classical machine learning metrics assume a prediction window of 1 day. This means that a UE is counted as successfully mitigated, i.e. as a true positive, if at least one mitigation action completed within the previous 24 hours, i.e. was initiated within the previous 24 hours minus the 2 node–minutes mitigation overhead specified in Section 3.2. The remaining UEs are counted as not mitigated, i.e. as false negatives. We only employ the prediction window to calculate the classical machine learning metrics, which need a binary classification into mitigated or not mitigated. The cost–benefit calculation uses the real UE and mitigation costs described in Section 4.3.

The number of mitigations is the number of times that the policy selects the mitigation action ($a = 1$ in the case of RL). A single UE may be mitigated multiple times within the 24-hour period, but only one of these mitigations (which can be imagined to be the one that happens last) is a true positive. The other mitigations are redundant and counted as false positives. The number of non-mitigations is the number of times that the policy selects not to mitigate ($a = 0$ for the RL agent) plus the number of UEs that have no event in the preceding time window of 1 day. If there is no event within the 24 hours before the UE, then none of the policies, all of which mitigate only in response to an event, has an opportunity to mitigate the UE. Nevertheless, since the UE was not mitigated, it must be counted as a false negative, to avoid biasing our results by ignoring the hardest-to-mitigate UEs. We avoid this bias by assuming that the system makes an implicit "no-mitigate" false negative action for these UEs.

Recall is the proportion of actual positives that are correctly identified as such. In our case, this metric refers to the fraction of UEs that are correctly predicted:

$$Recall = \frac{Correctly\ predicted\ UEs}{Total\ UEs\ occurred} = \frac{TPs}{TPs + FNs}$$

Precision refers to the percentage of observations classified as positives that are true positives. In our case, the precision refers to the ratio between correctly predicted/mitigated UEs and the total number of mitigations performed:

$$Precision = \frac{Correctly\ predicted\ UEs}{Total\ mitigations} = \frac{TPs}{TPs + FPs}$$

4.5 Generality to other job sizes

We increase the confidence in the generality of our method to different HPC system architectures and HPC job sizes. To consider different architectures, we partition the MareNostrum 3 error logs by DRAM manufacturer, generating three smaller subsystems, of size 6694, 5207 and 13,419 DIMMs, from anonymized Manufacturers A, B and C respectively. With few exceptions, all DIMMs in a given node are from the same DRAM manufacturer. Firstly, we trained and evaluated the method on the whole system, *MN/All*. Secondly, we performed separate training and testing for each subsystem comprising a single DIMM manufacturer: *MN/A*, *MN/B* and

MN/C. Finally, we give results for the sum of the three subsystems, *MN/ABC*, which differs from *MN/All* only because it uses three separately trained models.

To consider different HPC job sizes, we perform a job size sensitivity analysis. This is necessary because HPC jobs are known to differ in size and duration by orders of magnitude [23, 27, 48–50, 57, 70, 71]. We investigate the effect on the cost–benefit calculation of job sizes up to ten times smaller or ten times larger than those seen on MareNostrum 4. Future work could consider how the results would differ for cloud platforms, using the public datasets from Microsoft Azure [14] or Google Borg [69], or for other HPC systems using public logs [1] or synthetic trace generators [13].

4.6 Generality to other hosts and memory architectures

Our results are for a single supercomputer and memory system architecture (with three different vendors). To fully test the generality of our method, it is important to consider other CPU or GPU host architectures with different error correction schemes and error logging capabilities. It would also be interesting to analyze the impact of on-die ECC, as supported by current HPC DIMMs, which transparently corrects errors in the memory devices. On-die ECCs are not standardized by JEDEC or as part of the host–memory interfaces, so the impact could be very different for different manufacturers. Modern memory interfaces, HBM, DDR DIMMs and memory-over-CXL enable more heterogeneity in the memory system, which may also impact the results.

Our RL method is released as open source. Since it has no user-supplied parameters, the method can be applied without any customization or tuning to different host and memory system architectures. We encourage the community to evaluate the method on different systems and share their findings.

5 RESULTS

5.1 Cost–benefit analysis

Figure 3 shows the overall results of the cost–benefit analysis. The *y*-axis is the total cost over the two-year production time period, which is the sum of the cost of the UEs (solid color) and the cost of mitigations (with dashes), calculated as the sum across all six splits in the time series nested cross-validation (Section 4.1). The eight bars for each scenario correspond to the eight approaches described in Section 4.2. These are the two baseline policies, Never-mitigate and Always-mitigate (on every error-related event), the state-of-the-art SC20-RF policy with optimal and suboptimal threshold parameters, Myopic-RF (our adaptive extension of SC20-RF), the RL approach of this paper, and the optimal Oracle policy. Results are given for mitigation costs of 2, 5 and 10 node–minutes.

In all scenarios, the Never-mitigate policy has a large cost, underscoring the need for some kind of UE mitigation approach. Its cost is entirely due to UE costs, so it is independent of the mitigation cost, at 74,035 node–hours over the two-year production period. The simplest mitigation strategy, Always-mitigate, is effective for a small mitigation cost of 2 node–minutes, reducing the cost by 46% to 39,769 node–hours. It has the lowest possible UE cost for our dataset and approach triggered by events in the log, but also the highest mitigation cost, at 8642 node-hours. As the mitigation
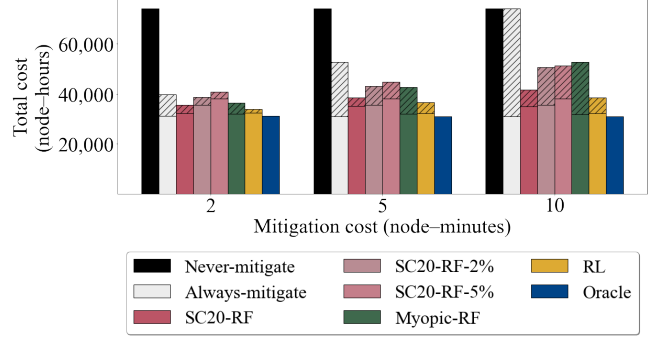

Figure 3: Total cost for MN/All, as the sum of UE cost (solid color) and mitigation cost (with dashes). The RL agent has lower total cost than the other approaches due to a much lower mitigation cost. Unlike SC20-RF it is not sensitive to a user-supplied parameter. The results are stable for mitigation costs between 2 node–minutes and 10 node–minutes.

cost increases, however, the cost of Always-mitigate increases dramatically, and for a cost of 10 node–minutes, it is slightly worse than Never-mitigate (see Section 5.6 for a sensitivity analysis using smaller and larger job sizes). Always-Mitigate implicitly includes a form of prediction, since "always" means that any kind of event in the log is treated as an indicator of an upcoming UE.

The random forest predictor of SC20-RF, with the optimal choice of the user-defined threshold parameter, reduces the total cost significantly. For a 2 node–minute mitigation cost, it reduces the cost by 52% compared to Never-mitigate to 35,543 node–hours. The decision threshold for SC20-RF needs to be selected carefully, as it significantly affects the machine learning metrics and cost–benefit analysis [11]. The results verify this, as with a SC20-RF threshold of just 2% (or 5%) from optimal, the total cost of SC20-RF increases to 38,645 (40,740) node–hours.

The Myopic-RF policy, while seeming to be a reasonable approach, has consistently worse results than SC20-RF. For a 2 node–minute mitigation cost, this increase is small, to 36,432 node–hours, but the gap widens considerably as the mitigation cost increases. The disappointing results for Myopic-RF arise because although the output from the RF predictor increases with the likelihood of error, it is not a reliable probability value, as assumed by Myopic-RF.

The RL approach consistently reduces the total cost to 54% below Never-mitigate, at 33,843 node–hours. For a 2 node–minute mitigation cost, the advance over SC20-RF is mainly due to the lower mitigation cost, which is approximately 55% lower than that of SC20-RF. As the mitigation cost increases, a better choice of when to apply mitigation gives a similar mitigation cost but somewhat lower total cost. Finally, the Oracle reduces the total cost by 58% to 31,129 node–hours. The negligible total mitigation cost of the Oracle shows that the mitigation cost of the other approaches is almost entirely unnecessary mitigations (false positives).

All results include the cost to train and validate the model, where applicable. The cost of SC20-RF is "on the order of node–minutes" [11] and the cost for RL is less than twenty node–hours per year. The RL agent has a greater training and validation cost
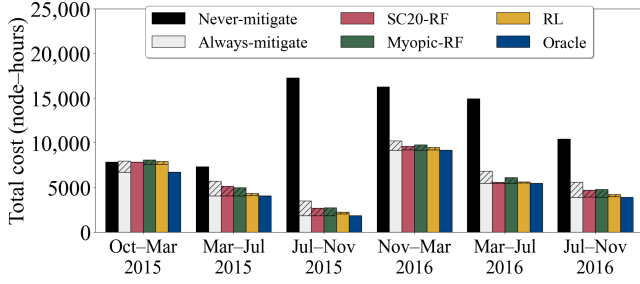
Figure 4: Time series nested cross-validation for MN/All with 2 node–minute mitigation cost, starting from untrained models. The total cost is the sum of UE cost (solid color) and mitigation cost (with dashes).
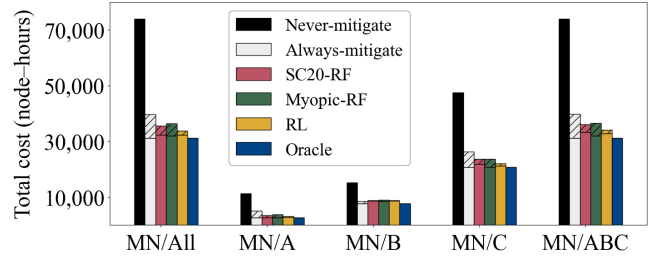

Figure 5: Total cost for the three anonymized DRAM manufacturers. Each bar is the sum of UE cost (solid color) and mitigation cost (with dashes). The RL agent has lower total cost than the other approaches due to a much lower mitigation cost. This result is consistent across all DRAM manufacturers.

than SC20-RF, but the difference is negligible compared with the additional saved node–hours. In addition, SC20-RF has a hidden cost to determine the optimal value of its threshold parameter. This cost is not quantified in our results, but it could be significant.

In summary, these results show that our RL approach, compared with the state-of-the-art SC20-RF, reduces the total cost by 5% and narrows the distance from the optimal Oracle by more than a third.

5.2 Time series nested cross-validation

Figure 4 shows the complete results from the time series cross-validation for MN/All. The y-axis is again the total cost. The x-axis is time, showing a separate set of results for each split, each of which corresponds to a roughly four-month period during the MareNostrum 3 operation. The sum across time of the values in Figure 4 match the 2 node–minute bars of Figure 3. We see that the relative performance of all six approaches is stable over time. In all six periods except the first, Never-mitigate consistently has the highest cost, showing a constant need for some kind of error mitigation throughout operation. SC20-RF outperforms Always-mitigate in all of the six periods, due to the much lower mitigation costs for a normally similar UE cost. Myopic-RF has higher cost than SC20-RF for all time periods except the second. Finally, RL matches SC20-RF, within 1.2%, for two periods and is the overall best realistic approach for four of the six periods, with up to 17% improvement over SC20-RF.

5.3 Different DRAM manufacturers

Figure 5 shows results for the three anonymized DRAM manufacturers and a mitigation cost of two node–minutes. As before, the y-axis is the total cost across the two-year production time period, as the sum of the costs of the UEs (solid) and mitigations (dashed). Separate results are shown for the whole system (MN/All), as well as per manufacturer (MN/A, MN/B and MN/C) and their sum (MN/ABC).

The relative effectiveness of the six approaches are broadly similar across all scenarios considered: whether applied and evaluated to MareNostrum 3 as a whole or separately to MN/A, MN/B and MN/C. The MN/ABC results are similar to those for MN/All, but slightly worse, likely because MN/All allows generalization among
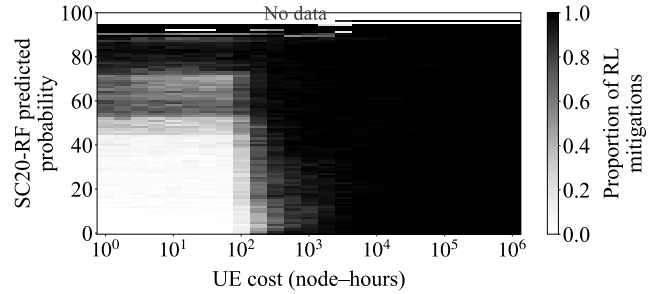

Figure 6: RL agent behavior: the shade indicates the fraction of events for which the agent triggers a mitigation as a function of the potential UE cost (x-axis) and the likelihood of a UE (y-axis) determined by the RF predictor.

manufacturers whereas MN/ABC does not. We see that RL is significantly better than SC20-RF for all scenarios except MN/B, for which the results are similar.

5.4 RL agent behavior

Figure 6 illustrates the behavior of the RL agent, which helps understand in which circumstances the agent decides to mitigate. The x-axis (log scale) is the UE cost input to the RL agent (Equation 3), which is the CPU time since the job start or the last checkpoint. The y-axis indicates the probability of a predictable UE. Our agent has no such probability value, whether as an input, intermediate value or output. As a proxy the y-axis therefore shows the probability output from the state-of-the-art random forest predictor (SC20-RF). This is not an input to the agent, but it does serve as a measure of the risk of an upcoming UE. The shade in the chart indicates how often the agent mitigates in those circumstances, with white meaning that it never mitigates and black that it always mitigates. The region at the top marked "No data" indicates that these datapoints are never seen during training. Each bin comprises the relevant training episodes in the last cross validation split.

For low potential UE costs, below about 100 node–hours, and low predicted UE probability, below about 50%, the agent initiates few mitigations (bottom-left part of the chart). As the UE cost

Table 2: Prediction results and classical machine learning metrics for the six approaches. The RL policy is the only approach that adapts to the current job characteristics, by more frequently performing mitigations when the cost of a UE would be high.

Approach	TPs	FNs	FPs	TNs	Mitigations (TPs+FPs)		Recall	Precision
Never-mitigate	0	67	0	259,228	0	(0%)	0%	*n/a*
Always-mitigate	42	25	259,228	0	259,270	(100%)	63%	0.02%
SC20-RF	40	27	96,612	162,616	96,652	(37%)	60%	0.04%
Myopic-RF	32	35	132,864	126,364	132,896	(51%)	48%	0.02%
RL								
MN4 job distribution	26	41	43,544	215,684	43,570	(17%)	39%	0.06%
UE cost < 100 node−hours	18	49	49,678	209,550	49,696	(19%)	27%	0.04%
100 ≤ UE cost < 1000 node−hours	29	38	86,722	172,506	86,751	(33%)	43%	0.03%
UE cost ≥ 1000 node−hours	41	26	240,155	19,073	240,196	(93%)	61%	0.02%
Oracle	42	25	0	259,228	42	(0%)	63%	100%

increases, the proportion of mitigations increases, with the agent usually triggering a mitigation when the UE cost is above about 1000 node−hours, even if the likelihood of a UE is low. Similarly, the agent usually initiates mitigations when the predicted probability is above about 70%. When the UE cost and likelihood of a UE are both high (top-right part of the chart), the mitigation is almost always performed.

Figure 6 also shows that the agent properly generalizes to very large potential UE costs. The training data contains a small number of UE costs exceeding 1000 node−hours, with a maximum of 32,000 node−hours. Nevertheless, the agent consistently chooses to always mitigate for one and two orders of magnitude greater costs.

5.5 Classical machine learning metrics

Table 2 shows the numbers of true positives (TPs), false negatives (FNs), false positives (FPs) and true negatives (TNs), as defined in Section 4.4, for all six approaches. It also shows the total number of mitigations, as well as recall and precision, which are derived from these numbers.

Never-mitigate never performs a mitigation action (positive), so it has zero TPs or FPs. Its recall, $TPs/(TPs + FNs)$, is therefore 0% and its precision, $TPs/(TPs + FPs)$, is undefined. Always-mitigate has 42 true positives, corresponding to the 42 UEs that have at least one event in the 1-day prediction window defined for the classical machine learning metrics. But 25 UEs have no event in the 1-day prediction window, so from the perspective of the classical machine learning metrics, they cannot be mitigated and are counted as false negatives. This leads to a recall of 63%, which is the best possible for all approaches that perform a mitigation only in response to an error event. Always-mitigate, however, has the lowest precision with a value of 0.02%, due to the high number of FPs (259,228). SC20-RF has a slightly lower recall than Always-mitigate, at 60%, but many fewer FPs, leading to a significantly improved precision of 0.04%. Compared with SC20-RF, Myopic-RF has a lower recall, at 48% and a lower precision, at 0.02%, due to the much lower number of TPs.

To understand the behavior of the RL policy in different conditions, we show separate results for the MareNostrum 4 job distribution (first row) and for three uniformly randomly distributed ranges of UE costs (three remaining rows). For the MareNostrum 4 job distribution (first row), the overall recall is much lower than

SC20-RF, at 39%, while the precision is much higher, at 0.06%. It may appear that the RL policy is making a poor tradeoff, due to the lower number of mitigated UEs (true positives), but this is not the case, as previously seen in the cost−benefit calculation. For UE costs less than 100 node−hours (second row), the agent requests mitigations only when there is either a high probability of a UE or a high potential UE cost. This leads to the lowest recall of 27% and a precision of 0.04%. While a higher recall would represent a greater number of predicted UEs, the relatively small cost of any UEs would be insufficient to justify the greater number of false positive mitigation actions. For UE costs between 100 and 1000 node−hours (third row), mitigation is performed more often, leading to a recall of 43% and a precision of 0.03%. Finally, for UE costs uniformly distributed between 1000 node−hours and the maximum job size of 32,000 node−hours (fourth row), RL behaves like Always-mitigate, leading to a recall of 61% (almost as high as 63% for Always-mitigate) and a precision of 0.02% (similar to Always-mitigate). Finally, the Oracle has the highest possible recall, of 63%, which is the same as Always-mitigate, and the highest possible precision, of 100%, since all mitigation actions are true positives.

With the exception of Oracle, which has the maximum value for both metrics, recall and precision, it is not possible to conclude, from these metrics alone, which policy is best. Firstly, precision considers TPs and FPs to have the same weight, when in reality they differ in cost by orders of magnitude. Secondly, there is generally a tradeoff between recall and precision, and an increase in one typically results in a decrease in the other. RL is the only policy that dynamically adjusts this tradeoff to optimize the cost−benefit calculation.

5.6 Job size sensitivity analysis

In order to verify the generality of our method on systems with different job sizes, we repeat the experiment with up to ten times smaller or ten times larger job sizes. Each experiment, for a different scaling factor, uses a separately trained model, which corresponds to the normal use case of training a model for the particular production system. The results are the average across all six splits in the time series nested cross-validation, for the complete system MN/All. In order to focus on the effect of job size, all results maintain the same 2 node−minute mitigation time as before.

Figure 7a shows the total cost of mitigations and UE errors (y-axis, log scale), as a function of the job size scaling factor (x-axis, also log scale). A scaling factor of 1 corresponds to the job distribution in the original MareNostrum 4 job log. As expected, the cost of the uncorrected errors, and therefore the benefits of error mitigation, both increase with the job scaling factor. Never-mitigate has total cost equal to the UE cost, which is directly proportional to the scaling factor. For scaling factors of 1, 3 and 10, Never-mitigate has total costs of 74,035, 222,104 and 740,346 node-hours respectively. Always-mitigate reduces the UE cost by a factor of about 2.4, independent of the scaling factor, but it adds a fixed mitigation cost of 8642 node–hours (see Section 5.1). For large scaling factors, its total cost is dominated by the UE cost and is therefore close to proportional to the scaling factor, about 2.4× lower than that of Never-mitigate. But for job scaling factors less than about 0.2, the high mitigation cost of Always-mitigate dominates and Never-mitigate becomes the best static baseline policy. On the large logarithmic scale covering two orders of magnitude, SC20-RF, Myopic-RF and RL appear similar. All always perform better than the static baseline policies, with the benefit of the prediction schemes largest for moderately smaller job sizes than those of MareNostrum 4. The RL-triggered mitigation policy has the lowest costs, of all policies except Oracle, at 32,391, 96,379 and 320,349 node-hours.

Figure 7b focuses on just the mitigation costs incurred by the different approaches, as the job sizes are scaled. The axes are the same as for Figure 7a, except that the y-axis now shows only the mitigation cost, in node–hours, on a linear scale. All three prediction-based approaches, SC20-RF, Myopic-RF and RL adapt to the job size scaling factor, by incurring a lower mitigation cost when the job sizes are smaller. For SC20-RF, this adaptation is done by the user somehow specifying a different optimal threshold parameter. In the case of Myopic-RF and the RL agent, this adaptation is done automatically. Nevertheless, we see that the RL agent consistently achieves a lower mitigation cost than the other realistic approaches.

Various studies from NERSC, NSF and US national labs report typical HPC job sizes that are two or three orders of magnitude larger than the jobs used in our evaluation [27, 41, 49, 57]. Given that we have verified the generality of our method with different job sizes, we argue that application of our method in these systems would lead to roughly proportional savings that are two to three orders of magnitude higher than our results for MareNostrum 3.

Numerous studies considering large-scale HPC systems report checkpointing overheads of tens of percents of the overall available node–hours [7, 9, 16, 21, 22, 45, 52, 54, 63], which is considerably higher than observed in our study. Driven by the needs of large-scale systems, optimizing the checkpointing interval to reduce overheads is an active area of research. To the best of our knowledge, our study is the first to propose and evaluate an RL adaptive mitigation scheme that would lead to significant system performance gains in HPC systems with a high failure mitigation cost.

5.7 Application completion times

Our study focuses on the system-level impact of DRAM failures and the potential for the system operator to reduce the number of lost node–hours. At the same time, error mitigation approaches can also improve the service delivered to individual users. Wang et al. [63]
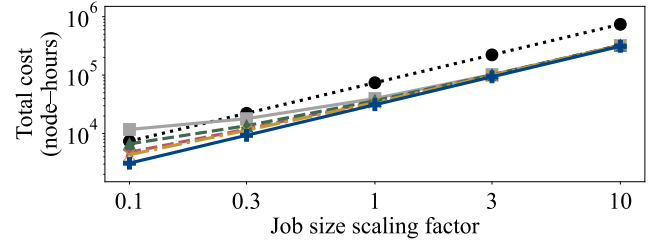
(a) Total cost in node–hours (UE plus mitigation cost). The RL approach has the lowest total cost among all realistic approaches across the whole range. The best static policy changes from Never-mitigate to Always-mitigate at about one-third the job cost of MareNostrum.
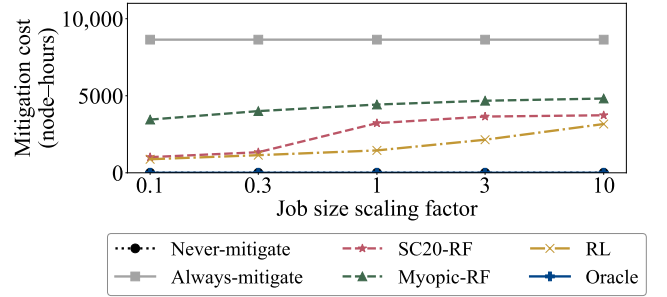
(b) Mitigation cost in node–hours. Never-mitigate, Always-mitigate and Oracle have fixed mitigation costs independent of the job sizes. SC20-RF adjusts to the job size through the external threshold parameter. Myopic-RF adapts to the job size scalefactor through the expected UE cost. RL automatically adjusts to the job size.

Figure 7: Sensitivity analysis for job size scaling factor.

and Elliott et al. [21] report an n-fold reduction in job wall-clock time, due to the deployment of checkpointing. The trade-off between false positives and false negatives motivates the exploration of adaptive mitigation policies that adjust to the job and system state. An interesting avenue of future work would be to analyze the application-level benefits of our proposal, considering application completion time and its variability under different mitigation approaches.

6 RELATED WORK

6.1 Corrected DRAM errors

Most of the earlier studies on the classification and prediction of memory errors focus on corrected DRAM errors [5, 6, 15, 18, 43, 44, 61]. These studies help to understand corrected DRAM error rates and distributions, and they identify correlations with various features that are useful for prediction. It is important, however, to determine how and to what extent this information could contribute to measurable improvements in system reliability. System reliability is only impacted by UEs [26, 38, 55, 74], and there is no direct relation between corrected and uncorrected error prediction [25, 35, 47, 56, 59, 74]. It is therefore challenging to modify an existing CE predictor to predict UEs [18].

6.2 Corrected vs. uncorrected DRAM errors

A few studies show that the probability of an uncorrected DRAM error is higher if the DIMM previously experienced corrected errors [56, 59, 74]. This reasoning is used by system protection mechanisms that try to prevent future uncorrected errors using simple heuristics to retire potentially failing memory pages [19, 30, 39, 62, 67] or replace the affected DIMMs [20, 28, 32, 38, 56]. The recent large-scale study of Cheng et al. [12], however concludes that UE failures are hard to predict, since typically only a small number of CEs occur before these failures and the CEs only manifest within a short time before the failures happen.

6.3 Uncorrected DRAM errors

The community has more recently applied advanced machine learning methods to predict uncorrected DRAM errors.

In a 2017 paper, Giurgiu et al. [25] present the first machine learning model to predict uncorrected DRAM errors. Their random forest model is based on preceding corrected errors and measurements from over 100 sensors that monitor the system. The model is designed and evaluated based on event logs from 49,800 IBM servers in multiple geographical locations during a period of over three years.

Mukhanov et al. [42] explore the importance of workload characteristics, such as IPC and memory bandwidth utilization, on the characterization and prediction of DRAM errors. The study is performed on a single server with 72 DRAM chips running under non-nominal circuit parameters: scaled refresh period, lowered voltage and increased temperature.

Workload-aware DRAM error prediction is further explored by Wang et al. [64] in a large-scale study of a cloud datacenter comprising 382,608 servers. three tree-based models. The results show that considering the workload's used memory bandwidth and latency improves upon a baseline prediction based only on the platform characteristics, the number of CEs and their location.

These error prediction models are evaluated using standard evaluation metrics, such as precision and recall. Such metrics allow comparison with the state of the art in machine learning, but they do not allow us to conclude how well the predictor would serve to reduce the costs of UE errors. Metrics like precision put the same weight on multiple different prediction outcomes (true/false positives/negatives), whose costs differ by orders of magnitude, and the recall metric ignores false positives, which incur costly mitigation measures. Overall, these standard data prediction metrics are insufficient to evaluate HPC failure predictors, and their use should be complemented with a cost–benefit analysis.

Boixaderas et al. [11] is the first study that performs such an analysis. It compares the system resources needed for model training, failure prediction and mitigation against the compute time that is saved by successful failure mitigation. The study develops and compares six machine learning classifiers and it proposes an error prediction method based on random forest. The method is trained and evaluated using logs from the MareNostrum supercomputer.

Two recent studies from Internet servers and the cloud domain use a similar cost–benefit calculation for DRAM failure prediction. Li et al. [36] analyze DRAM errors from a ByteDance Internet facility comprising around 100,000 Intel SkyLake and Cascade Lake servers. The study proposes three simple UE predictors based on the CE history and the details of the system's ECC algorithms to predict the risky CEs. The ECC can correct risky CE patterns with limited assured coverage, so a small variation in a risky CE will likely result in a UE. The authors show cost–benefit improvements when risky CE patterns are considered.

Zhang et al. [73] predict the loss of node availability due to DRAM failures for the Alibaba Cloud Elastic Compute Service with more than half a million nodes. In addition to UEs, the study also analyzes node unavailability caused by CE storms, high CE rates that saturate system error handling mechanism and cause a node to become unresponsive. The authors predict DRAM-caused system failures based on a 18 heuristic rules combined with four binary classification ML models.

The three previous studies create static prediction models that don't adapt to the current state of the system. This is problematic in high-performance computing because the failure cost varies among jobs whose size and duration can differ by orders of magnitude. Our method dynamically adapts to the current system state, learning a policy that takes account of the running job characteristics. By avoiding mitigation actions when the cost of a UE would be low, it reduces the total cost by 5%, in comparison with Boixaderas et al., which uses similar logs from the same supercomputer as our study.

7 CONCLUSIONS

This paper presented and evaluated a reinforcement learning method that anticipates and triggers the mitigation of DRAM uncorrected errors. The method is trained and evaluated using two years of production error and job logs from the MareNostrum supercomputer. Our cost–benefit analysis shows that the adaptive mitigation method reduces the lost compute time by 54%, an overall saving of 20,000 node–hours per year. By adapting to the current job size, rather than using a static cost estimate, the saved node–hours is just 6% below the optimal Oracle method, reducing the distance from optimal by more than a third compared with the state-of-the-art random forest method. We verify the generality with different job sizes and argue that application of our method on larger HPC systems with larger HPC job sizes would lead to roughly proportional savings two to three orders of magnitude higher than observed on MareNostrum.

All source code is released as open source. Since the method has no user-supplied parameters, it can be easily applied to other large-scale clusters without customization or tuning. We would encourage the community to evaluate and further improve the method on their systems and share their findings.

8 ACKNOWLEDGMENTS

REFERENCES

[1] [n. d.]. Logs of Real Parallel Workloads from Production Systems. https://www.cs.huji.ac.il/labs/parallel/workload/logs.html.

[2] [n. d.]. Partnership for Advanced Computing in Europe (PRACE) Research Infrastructure. http://www.prace-ri.eu.

[3] Barcelona Supercomputing Center. 2016. *MareNostrum 3 User's Guide*.

[4] Barcelona Supercomputing Center. 2017. *MareNostrum 4 (2017) System Architecture*. https://www.bsc.es/marenostrum/marenostrum/technical-information.

[5] Elisabeth Baseman, Nathan DeBardeleben, Kurt Ferreira, Scott Levy, Steven Raasch, Vilas Sridharan, Taniya Siddiqua, and Qiang Guan. 2016. Improving DRAM Fault Characterization through Machine Learning. In *International Conference on Dependable Systems and Networks Workshop (DSN-W)*. 250–253.

[6] Elisabeth Baseman, Nathan DeBardeleben, Kurt B. Ferreira, Vilas Sridharan, Taniya Siddiqua, and Olena Tkachenko. 2017. Automating DRAM Fault Mitigation By Learning From Experience. In *International Conference on Dependable Systems and Networks Workshops, (DSN-W)*. 137–140.

[7] Leonardo Bautista-Gomez, Seiji Tsuboi, Dimitri Komatitsch, Franck Cappello, Naoya Maruyama, and Satoshi Matsuoka. 2011. FTI: High performance fault tolerance interface for hybrid systems. In *International Conference for High Performance Computing, Networking, Storage, and Analysis (SC)*. 1–32.

[8] Richard Bellman. 1957. A Markovian decision process. *Journal of mathematics and mechanics* 6, 5 (1957), 679–684.

[9] Keren Bergman, Shekhar Borkar, Dan Campbell, William Carlson, William Dally, Monty Denneau, Paul Franzon, William Harrod, Kerry Hill, Jon Hiller, et al. 2008. Exascale computing study: Technology challenges in achieving exascale systems. *Defense Advanced Research Projects Agency Information Processing Techniques Office (DARPA IPTO), Tech. Rep* 15 (2008), 181.

[10] Isaac Boixaderas, Sergi Moré, Javier Bartolome, David Vicente, Petar Radojković, Paul M. Carpenter, and Eduard Ayguadé. 2024. UERL: A method for mitigating DRAM Uncorrected Errors using Reinforcement Learning. https://doi.org/TODO

[11] Isaac Boixaderas, Darko Zivanovic, Sergi Moré, Javier Bartolome, David Vicente, Marc Casas, Paul M. Carpenter, Petar Radojković, and Eduard Ayguadé. 2020. Cost-Aware Prediction of Uncorrected DRAM Errors in the Field. In *International Conference for High Performance Computing, Networking, Storage and Analysis (SC)*. 1–15.

[12] Zhinan Cheng, Shujie Han, Patrick PC Lee, Xin Li, Jiongzhou Liu, and Zhan Li. 2022. An In-Depth Correlative Study Between DRAM Errors and Server Failures in Production Data Centers. In *International Symposium on Reliable Distributed Systems (SRDS)*.

[13] Walfredo Cirne and Francine Berman. 2001. A comprehensive model of the supercomputer workload. In *IEEE International Workshop on Workload Characterization*.

[14] Eli Cortez, Anand Bonde, Alexandre Muzio, Mark Russinovich, Marcus Fontoura, and Ricardo Bianchini. 2017. Resource central: Understanding and Predicting Workloads for Improved Resource Management in Large Cloud Platforms. In *Symposium on Operating Systems Principles*. 153–167.

[15] Carlos H. A. Costa, Yoonho Park, Bryan S. Rosenburg, Chen-Yong Cher, and Kyung Dong Ryu. 2014. A System Software Approach to Proactive Memory-Error Avoidance. In *International Conference for High Performance Computing, Networking, Storage and Analysis (SC)*. 707–718.

[16] John T Daly, Lori A Pritchett-Sheats, and Sarah Ellen Michalak. 2008. Application MTTFE vs. platform MTBF: A fresh perspective on system reliability and application throughput for computations at scale. In *IEEE International Symposium on Cluster Computing and the Grid (CCGRID)*. 795–800.

[17] Anwesha Das, Frank Mueller, Paul Hargrove, Eric Roman, and Scott Baden. 2018. Doomsday: Predicting Which Node Will Fail When on Supercomputers. In *International Conference for High Performance Computing, Networking, Storage, and Analysis (SC)*. Article 9, 14 pages.

[18] Xiaoming Du and Cong Li. 2018. Memory Failure Prediction Using Online Learning. In *International Symposium on Memory Systems (MEMSYS)*. 38–49.

[19] Xiaoming Du, Cong Li, Shen Zhou, Xian Liu, Xiaohan Xu, Tianjiao Wang, and Shijian Ge. 2021. Fault-Aware Prediction-Guided Page Offlining for Uncorrectable Memory Error Prevention. In *International Conference on Computer Design (ICCD)*.

[20] Xiaoming Du, Cong Li, Shen Zhou, Mao Ye, and Jing Li. 2020. Predicting Uncorrectable Memory Errors for Proactive Replacement: An Empirical Study on Large-Scale Field Data. In *European Dependable Computing Conference (EDCC)*.

[21] James Elliott, Kishor Kharbas, David Fiala, Frank Mueller, Kurt Ferreira, and Christian Engelmann. 2012. Combining partial redundancy and checkpointing for HPC. In *2012 IEEE 32nd International Conference on Distributed Computing Systems*. IEEE, 615–626.

[22] Mootaz Elnozahy. 2009. System resilience at extreme scale: A white paper. *DARPA Resilience Report for ITO, William Harrod* (2009).

[23] Yuping Fan, Zhiling Lan, Taylor Childers, Paul Rich, William Allcock, and Michael E Papka. 2021. Deep Reinforcement Agent for Scheduling in HPC. In *IEEE International Parallel and Distributed Processing Symposium (IPDPS)*. 807–816.

[24] Alvaro Frank, Manuel Baumgartner, Reza Salkhordeh, and André Brinkmann. 2021. Improving checkpointing intervals by considering individual job failure probabilities. In *IEEE International Parallel and Distributed Processing Symposium (IPDPS)*. 299–309.

[25] Ioana Giurgiu, Jacint Szabo, Dorothea Wiesmann, and John Bird. 2017. Predicting DRAM Reliability in the Field with Machine Learning. , 15–21 pages.

[26] Saurabh Gupta, Tirthak Patel, Christian Engelmann, and Devesh Tiwari. 2017. Failures in Large Scale Systems: Long-term Measurement, Analysis, and Implications. In *International Conference for High Performance Computing, Networking, Storage and Analysis (SC)*. 44:1–44:12.

[27] David Hart. 2011. Deep and wide metrics for HPC resource capability and project usage. In *International Conference for High Performance Computing, Networking, Storage and Analysis (SC)*. 1–7.

[28] Hewlett Packard Enterprise 2016. *HPE ProLiant DL580 Gen9 Server User Guide*. Hewlett Packard Enterprise.

[29] HP. 2016. *How memory RAS technologies can enhance the uptime of HPE ProLiant servers*. Technical white paper 4AA4-3490ENW. Hewlett Packard Enterprise.

[30] Andy A. Hwang, Ioan A. Stefanovici, and Bianca Schroeder. 2012. Cosmic Rays Don't Strike Twice: Understanding the Nature of DRAM Errors and the Implications for System Design. In *International Conference on Architectural Support for Programming Languages and Operating Systems (ASPLOS)*.

[31] IBM 2014. *System x iDataPlex dx360 M4 Types 7912 and 7913: Problem Determination and Service Guide*. IBM.

[32] Intel Server Products and Solutions 2017. *System Event Log (SEL) Troubleshooting Guide*. Intel Server Products and Solutions.

[33] Kamil Iskra, John W Romein, Kazutomo Yoshii, and Pete Beckman. 2008. ZOID: I/O-forwarding infrastructure for petascale architectures. In *Proceedings of the 13th ACM SIGPLAN Symposium on Principles and practice of parallel programming*. 153–162.

[34] Andy Kleen. 2010. MCELOG: Memory Error Handling in User Space. In *International Linux System Technology Conference (Linux Kongress)*.

[35] Scott Levy, Kurt B. Ferreira, Nathan DeBardeleben, Taniya Siddiqua, Vilas Sridharan, and Elisabeth Baseman. 2018. Lessons Learned from Memory Errors Observed over the Lifetime of Cielo. In *International Conference for High Performance Computing, Networking, Storage, and Analysis (SC)*.

[36] Cong Li, Yu Zhang, Jialei Wang, Hang Chen, Xian Liu, Tai Huang, Liang Peng, Shen Zhou, Lixin Wang, and Shijian Ge. 2022. From Correctable Memory Errors to Uncorrectable Memory Errors: what Error Bits Tell. In *International Conference for High Performance Computing, Networking, Storage and Analysis (SC)*. 1093–1106.

[37] Xin Li, Michael C. Huang, Kai Shen, and Lingkun Chu. 2010. A Realistic Evaluation of Memory Hardware Errors and Software System Susceptibility. In *USENIX Conference on USENIX Annual Technical Conference (USENIXATC)*.

[38] Catello Di Martino, Zbigniew Kalbarczyk, Ravishankar K. Iyer, Fabio Baccanico, Joseph Fullop, and William Kramer. 2014. Lessons Learned from the Analysis of System Failures at Petascale: The Case of Blue Waters. In *International Conference on Dependable Systems and Networks (DSN)*. 610–621.

[39] Justin Meza, Qiang Wu, Sanjeev Kumar, and Onur Mutlu. 2015. Revisiting Memory Errors in Large-Scale Production Data Centers: Analysis and Modeling of New Trends from the Field. In *IEEE/IFIP International Conference on Dependable Systems and Networks (DSN)*. 415–426.

[40] Volodymyr Mnih, Koray Kavukcuoglu, David Silver, Alex Graves, Ioannis Antonoglou, Daan Wierstra, and Martin Riedmiller. 2013. Playing Atari with Deep Reinforcement Learning. *arXiv preprint arXiv:1312.5602* (2013).

[41] Adam Moody, Greg Bronevetsky, Kathryn Mohror, and B de Supinski. 2010. *Detailed modeling, design, and evaluation of a scalable multilevel checkpointing system, Lawrence Livermore National Laboratory (LLNL)*. Technical Report. Technical Report LLNL-TR-440491, July 2010.

[42] Lev Mukhanov, Konstantinos Tovletoglou, Hans Vandierendonck, Dimitrios S Nikolopoulos, and Georgios Karakonstantis. 2019. Workload-Aware DRAM Error Prediction using Machine Learning. In *IEEE International Symposium on Workload Characterization (IISWC)*. 106–118.

[43] Bin Nie, Devesh Tiwari, Saurabh Gupta, Evgenia Smirni, and James H Rogers. 2016. A large-scale study of soft-errors on GPUs in the field. In *IEEE International Symposium on High Performance Computer Architecture (HPCA)*.

[44] Bin Nie, Ji Xue, Saurabh Gupta, Tirthak Patel, Christian Engelmann, Evgenia Smirni, and Devesh Tiwari. 2018. Machine Learning Models for GPU Error Prediction in a Large Scale HPC System. In *International Conference on Dependable Systems and Networks (DSN)*.

[45] Ron A Oldfield, Sarala Arunagiri, Patricia J Teller, Seetharami Seelam, Maria Ruiz Varela, Rolf Riesen, and Philip C Roth. 2007. Modeling the impact of checkpoints on next-generation systems. In *Conference on Mass Storage Systems and Technologies (MSST 2007)*. 30–46.

[46] Adam J Oliner, Ramendra K Sahoo, José E Moreira, and Manish Gupta. 2005. Performance implications of periodic checkpointing on large-scale cluster systems. In *IEEE International Parallel and Distributed Processing Symposium*. 8–pp.

[47] Petar Radojkovic, Manolis Marazakis, Paul Carpenter, Reiley Jeyapaul, Dimitris Gizopoulos, Martin Schulz, Adria Armejach, Eduard Ayguade, François Bodin, Ramon Canal, et al. 2020. Towards resilient EU HPC systems: A blueprint.

[48] Gonzalo P. Rodrigo, Per-Olov Östberg, Erik Elmroth, Katie Antypas, Richard Gerber, and Lavanya Ramakrishnan. 2016. Tog Job Heterogeneity in HPC: A NERSC Case Study. In *IEEE/ACM International Symposium on Cluster, Cloud and Grid Computing (CCGrid)*. 521–526.

[49] Gonzalo P. Rodrigo, P-O Östberg, Erik Elmroth, Katie Antypas, Richard Gerber, and Lavanya Ramakrishnan. 2018. Towards understanding HPC users and systems: A NERSC case study. *J. Parallel and Distrib. Comput.* 111 (2018), 206–221.

[50] Gonzalo Pedro Rodrigo Álvarez, Per-Olov Östberg, Erik Elmroth, Katie Antypas, Richard Gerber, and Lavanya Ramakrishnan. 2015. HPC System Lifetime Story: Workload Characterization and Evolutionary Analyses on NERSC Systems. In *International Symposium on High-Performance Parallel and Distributed Computing.* 57–60.

[51] Rob Ross, Jose Moreira, Kim Cupps, and Wayne Pfeiffer. 2006. Parallel I/O on the IBM blue gene/L system. *Blue Gene/L Consortium Quarterly Newsletter, Tech. Rep., First Quarter* (2006).

[52] Kento Sato, Naoya Maruyama, Kathryn Mohror, Adam Moody, Todd Gamblin, Bronis R de Supinski, and Satoshi Matsuoka. 2012. Design and modeling of a non-blocking checkpointing system. In *International Conference for High Performance Computing, Networking, Storage, and Analysis (SC).* 1–10.

[53] Tom Schaul, John Quan, Ioannis Antonoglou, and David Silver. 2015. Prioritized Experience Replay. *arXiv preprint arXiv:1511.05952* (2015).

[54] Bianca Schroeder and Garth A Gibson. 2007. Understanding failures in petascale computers. In *Journal of Physics: Conference Series*, Vol. 78. IOP Publishing, 012022.

[55] Bianca Schroeder and Garth A. Gibson. 2010. A Large-Scale Study of Failures in High-Performance Computing Systems. *IEEE Transactions on Dependable and Secure Computing* 7, 4 (Oct 2010), 337–350.

[56] Bianca Schroeder, Eduardo Pinheiro, and Wolf-Dietrich Weber. 2009. DRAM Errors in the Wild: A Large-scale Field Study. In *International Joint Conference on Measurement and Modeling of Computer Systems (SIGMETRICS).* 193–204.

[57] Nikolay A Simakov, Joseph P White, Robert L. DeLeon, Steven M. Gallo, Matthew D. Jones, Jeffrey T. Palmer, Benjamin Plessinger, and Thomas R. Furlani. 2018. A Workload Analysis of NSF's Innovative HPC Resources Using XDMoD. *arXiv preprint arXiv:1801.04306* (2018).

[58] Vilas Sridharan, Nathan DeBardeleben, Sean Blanchard, Kurt B. Ferreira, Jon Stearley, John Shalf, and Sudhanva Gurumurthi. 2015. Memory Errors in Modern Systems: The Good, The Bad, and The Ugly. In *International Conference on Architectural Support for Programming Languages and Operating Systems (ASPLOS).* 297–310.

[59] Vilas Sridharan and Dean Liberty. 2012. A Study of DRAM Failures in the Field. In *International Conference on High Performance Computing, Networking, Storage and Analysis (SC).* Article 76, 76:1–76:11 pages.

[60] Vilas Sridharan, Jon Stearley, Nathan DeBardeleben, Sean Blanchard, and Sudhanva Gurumurthi. 2013. Feng Shui of Supercomputer Memory: Positional Effects in DRAM and SRAM Faults. In *International Conference on High Performance Computing, Networking, Storage and Analysis (SC).* Article 22, 22:1–22:11 pages.

[61] Xiaoyi Sun, Krishnendu Chakrabarty, Ruirui Huang, Yiquan Chen, Bing Zhao, Hai Cao, Yinhe Han, Xiaoyao Liang, and Li Jiang. 2019. System-Level Hardware Failure Prediction Using Deep Learning. In *56th Annual Design Automation Conference (DAC).* Article 20, 6 pages.

[62] Dong Tang, Peter Carruthers, Zuheir Totari, and Michael W. Shapiro. 2006. Assessment of the Effect of Memory Page Retirement on System RAS Against Hardware Faults. In *International Conference on Dependable Systems and Networks (DSN).*

[63] Chao Wang, Frank Mueller, Christian Engelmann, and Stephen L Scott. 2010. Hybrid checkpointing for MPI jobs in HPC environments. In *International Conference on Parallel and Distributed Systems.* 524–533.

[64] Xingyi Wang, Yu Li, Yiquan Chen, Shiwen Wang, Yin Du, Cheng He, YuZhong Zhang, Pinan Chen, Xin Li, Wenjun Song, et al. 2021. On Workload-Aware DRAM Failure Prediction in Large-Scale Data Centers. In *IEEE 39th VLSI Test Symposium (VTS).* 1–6.

[65] Ziyu Wang, Tom Schaul, Matteo Hessel, Hado Hasselt, Marc Lanctot, and Nando Freitas. 2016. Dueling Network Architectures for Deep Reinforcement Learning. In *International Conference on Machine Learning.* 1995–2003.

[66] Christopher John Cornish Hellaby Watkins. 1989. *Learning from Delayed Rewards.* Ph. D. Dissertation. King's College, Cambridge, UK. http://www.cs.rhul.ac.uk/~chrisw/new_thesis.pdf

[67] David Watts, Rani Doughly, and Ilya Solovyev. 2018. *Lenovo System x3850 X6 and x3950 X6 Planning and Implementation Guide.* Lenovo Press.

[68] Shimon Whiteson, Brian Tanner, Matthew E Taylor, and Peter Stone. 2011. Protecting Against Evaluation Overfitting in Empirical Reinforcement Learning. In *Symposium on Adaptive Dynamic Programming and Reinforcement Learning (ADPRL).* 120–127.

[69] John Wilkes. 2020. Yet more Google compute cluster trace data. Google research blog. Posted at https://ai.googleblog.com/2020/04/yet-more-google-compute-cluster-trace.html.

[70] Nicole Wolter, Michael O McCracken, Allan Snavely, Lorin Hochstein, Taiga Nakamura, and Victor Basili. 2006. What's Working in HPC: Investigating HPC User Behavior and Productivity. *CTWatch Quarterly* 2, 4A (2006), 9–17.

[71] Xu Yang, Zhou Zhou, Sean Wallace, Zhiling Lan, Wei Tang, Susan Coghlan, and Michael E Papka. 2013. Integrating dynamic pricing of electricity into energy aware scheduling for HPC systems. In *International Conference on High Performance Computing, Networking, Storage and Analysis (SC).* 1–11.

[72] Andy B. Yoo, Morris A. Jette, and Mark Grondona. 2003. Slurm: Simple Linux Utility for Resource Management. In *Workshop on job scheduling strategies for parallel processing.* 44–60.

[73] Pengcheng Zhang, Yunong Wang, Xuhua Ma, Yaoheng Xu, Bin Yao, Xudong Zheng, and Linquan Jiang. 2022. Predicting DRAM-Caused Node Unavailability in Hyper-Scale Clouds. In *International Conference on Dependable Systems and Networks (DSN).* 275–286.

[74] Darko Zivanovic, Pouya Esmaili Dokht, Sergi Moré, Javier Bartolome, Paul M. Carpenter, Petar Radojković, and Eduard Ayguadé. 2019. DRAM Errors in the Field: A Statistical Approach. In *International Symposium on Memory Systems (MEMSYS).*